Holographic Imaging of Atoms Using Thermal Neutrons

L. Cser and Gy. Török
Central Research Institute for Physics, Budapest P.O.B. 49, H-1525, Hungary

G. Krexner
Institute of Experimental Physics, University of Vienna, Boltzmanngasse 5, A-1090 Vienna, Austria

I. Sharkov
St. Petersburg State University, Institute of Physics, Chair of Optics and Spectroscopy, Ulyanovskaja Street 1, 198904 St. Petersburg, Russia

B. Faragó
Institut Laue-Langevin, 6 rue Jules Horowitz, BP 156-38042 Grenoble Cedex 9, France
(Received 23 July 2002; published 8 October 2002)

In a recent paper [L. Cser, G. Krexner, and Gy. Török, Europhys. Lett. **54**, 747 (2001)] the use of thermal neutrons with wavelengths close to interatomic distances in condensed matter was proposed to obtain holographic images on an atomic scale. Two experimental methods were considered which either put the radiation source inside and the detector outside the object or vice versa. The second approach, called the inside-detector concept, requires strongly neutron-absorbing isotopes acting as pointlike detectors in the sample. In the present work, we demonstrate the feasibility of this technique by recording a holographic image of a lead nuclei in a Pb(Cd) single crystal.

DOI: 10.1103/PhysRevLett.89.175504 PACS numbers: 61.12.–q

The idea of holographic imaging had been conceived by Denis Gabor already more than half a century ago [1], however, was successfully applied only more than two decades later as one of the striking consequences of the development of laser technology. For a long time holography was restricted to essentially the wavelength range of visible light causing an inherent limitation to the resolution obtainable in recording a hologram. A serious effort to extend holographic techniques to shorter wavelengths allowing for better resolution was made only during the past ten years when the development of both electron [2] and x-ray holography [3] made it possible for the first time to image objects on the scale of single atoms. Yet, applications of these techniques are still limited: In the case of electrons, their strong interaction with condensed matter restricts them largely to the investigation of surfaces. X-rays, on the other hand, while being able to penetrate more deeply into matter exhibit variations of sensitivity covering several orders of magnitude over the periodic table and thus impede their use for many systems involving particular combinations of elements. Neutrons, in principle, are not subject to these drawbacks. However, for various reasons mostly related to the limited intensity of presently available neutron beams, their application was not considered feasible. Only recently [4], three of the present authors put forward experimental setups permitting one to transfer certain conceptions developed in the context of x-ray holography to the case of neutrons: In the first of two approaches discussed, known as the inside-source concept, nuclei such as hydrogen exhibiting large incoherent neutron scattering cross sections serve as pointlike sources of neutron spherical waves. In contrast to that, the inside-detector concept interchanges the positions of source and detector as suggested by the principle of optical reciprocity. It can be realized by using strongly neutron-absorbing isotopes acting as pointlike detectors in the sample. Our inside-source concept for neutrons has been successfully applied recently [5].

Holographic imaging techniques are based on the recording of the interference pattern of two coherent waves emitted by the same source. The first wave that reaches the detector directly serves as the reference wave; the second one is scattered by the object of interest and subsequently interferes with the reference wave. For thermal neutrons, the realization of the inside-detector concept is based on the following considerations: A well collimated neutron beam, i.e., a plane wave, propagates towards a sample which is a single crystal containing a small amount of atoms whose nuclei are strongly neutron absorbing. The neutron wave reaches these detector nuclei either directly, without any scattering (and may thus serve as the reference beam), or after scattering from other nuclei in the sample. This latter process gives rise to the object beam. The intensity distribution of neutron radiation inside the crystal and, in particular, at the sites of the detector nuclei results from the interference between these two waves. The probability of absorption in a detector nucleus is proportional to the intensity of the neutron wave field at the position of this nucleus and, therefore, the number of absorption processes observed is directly related to the pattern resulting from the

interference of the object wave and the reference wave. The new nucleus emerging from the absorption process of a neutron by a detector nucleus is forming in an excited state and its subsequent transition to the ground state gives rise to the emission of γ radiation. The intensity of this γ radiation is directly proportional to the neutron intensity at the lattice sites of the detector nuclei. If recorded as a function of the sample orientation relative to the direction of the incident neutron beam this intensity pattern yields a hologram [4].

In the present work, a spherically shaped single crystal of $Pb_{0.9974}Cd_{0.0026}$ with a diameter of about 7 mm was used as the sample. In the case of Cd, the absorption cross section for thermal neutrons is more than 4 orders of magnitude larger than for Pb so that the Cd atoms act as highly efficient detectors. The phase diagram [6] shows that the crystal structure of the alloy is face-centered cubic (fcc) as for pure lead. Prior to the experiment, the quality of the single crystal was checked at the Laboratoire Léon Brillouin (Saclay, France), where it was confirmed that the crystal consisted of one single domain exhibiting a mosaicity of about 1.5°. The lattice parameter is $a = 4.935$ Å in good agreement with the values given in the literature [6]. The Cd atoms are randomly distributed on regular lattice sites. In an fcc lattice, every atom has 12 nearest neighbors and, since the Cd concentration is very low, usually all lattice sites surrounding any one Cd atom are occupied by Pb atoms. The lead nuclei play the role of the object while the cadmium nuclei serve as pointlike detectors inside the sample. The experiment was carried out at the D9 four-circle diffractometer installed at the high-flux research reactor of the Institute Laue-Langevin (Grenoble). The sample was mounted on the cradle of the diffractometer in such a way that the plane of the cradle was parallel to the incident beam. The sample was rotated about the angle χ through a range of 45° and about the angle φ through a range of 354°. The angular step width was 3° for both rotations leading to a mesh of $16 \times 119 = 1904$ pixels. Neutrons with a wavelength of $\lambda = 0.8397$ Å were obtained from a Cu (220) monochromator. Calibration based on the activation of a gold foil yielded a neutron flux close to 4.5×10^6 neutrons $\mathrm{cm}^{-2}\,\mathrm{s}^{-1}$ at the sample position (the hot source of the ILL reactor was not in operation during the time of the present experiment). The prompt γ rays emitted by the Cd nuclei were detected using two scintillation detectors shielded against the background from other sources (which is considerable in the reactor hall) by approximately 20 cm of lead. The two detectors were of different type and placed on opposite sides of the sample in order to facilitate identification of spurious intensity modulations. The data measured by the two detectors were evaluated separately. Two small holes (diameter about 2 cm) served as windows at the front side of the detectors facing the sample. One detector was a 3 in. × 3 in. NaI(Tl) scintillator, the second one a 2 in. × 2in. BGO scintillator. The sample-detector distance in both cases was about 7 cm. The count rate of the NaI(Tl) scintillator was about 2/3 of the count rate of the BGO detector. The discrimination threshold was set above the K_α x-ray energy of lead and all γ rays with higher energies were registered. A ^{3}He gas-filled proportional counter was placed close to the monochromator shielding in order to monitor the neutron flux during the experiment with sufficient accuracy. A tube with a length of 1 m containing a series of six progressively narrowing ring-shaped diaphragms was inserted in front of the sample thereby reducing the beam diameter from 20 to 10 mm. The diaphragms were machined from special polymer sheets containing admixtures of the strongly neutron-absorbing isotope ^{6}Li which was chosen because it does not emit any γ radiation following neutron capture. Likewise, where necessary, other parts of the experimental setup were covered with polymer foil containing ^{6}Li. The signal-to-noise ratio was slightly above 25. In order to decrease the influence of slow variations of the incident beam intensity, the measuring time for one pixel was limited to 30 sec. Short-time variations were registered by the monitor counter whose count rate was twice as high as the count rate of the BGO and 3 times as large as that of the NaI(Tl) detector. The data collection time for a full cycle, i.e., the time needed to cover the entire mesh of 1904 pixels, amounted to about 18 h. During the course of the experiment, 14 cycles were completed resulting in typically 2.5×10^7 counts in one pixel for the BGO and 1.5×10^7 counts for the NaI(Tl) detector. Figure 1 shows the data representing the hologram after normalization with the monitor counter and corrected for the slowly varying background level which was achieved by filtering out Fourier components of very low frequency and fitting a smoothly varying function to the spectra.

For reconstructing the object, computer-generated spherical waves were applied to the recorded hologram, i.e., convolution of converging s waves with the data matrix of the scanned (χ, φ) surface was carried out. The pattern obtained by this procedure gives the restored holographic picture. The sharp Kossel lines and

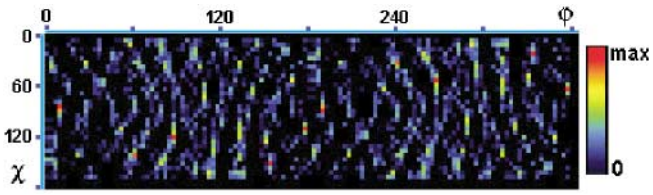

FIG. 1 (color). Raw hologram data plotted as a pixel map, each pixel covering 3° × 3° in the angular coordinates χ and φ, respectively. The column at the right side shows the range of holographic modulation (max= 120 000). The twofold symmetry of the crystal was used to double the χ range of the angular map.

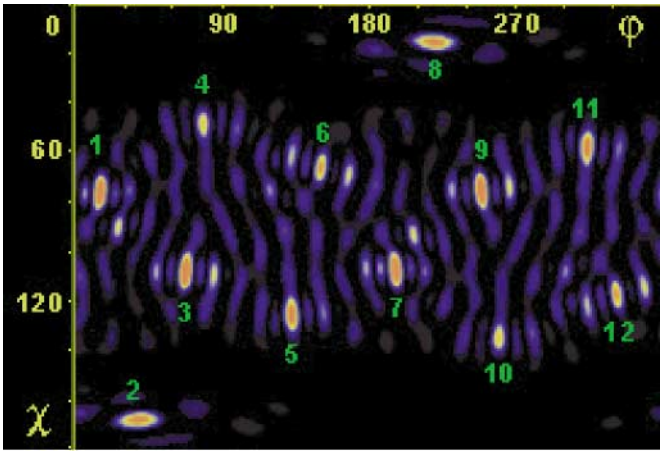

FIG. 2 (color). Reconstructed hologram of twelve Pb neighbors of a Cd nucleus in χ and φ coordinates. The intensity variation of the spots is due to the limited accuracy of the background approximation procedure. Nevertheless, the positions of all first neighbor Pb nuclei are clearly visible. The χ and φ coordinates of the spots (given in degrees) are as follows: 1. (78, 24); 2. (165, 45); 3. (72, 108); 4. (53, 84); 5. (123, 135); 6. (69, 156); 7. (107, 202); 8. (18, 225); 9. (77, 252); 10. (132, 264); 11. (62, 317); 12. (114, 335).

the contributions from nuclei at a greater distance than the first neighbors were filtered out by a smoothing algorithm included in the restoring procedure whose result is shown in Fig. 2. It can be seen that the spots of high intensity are not arranged in horizontal rows meaning that the [001] direction of the crystal lattice of the sample is not aligned along the z axis of the diffractometer. Since in an fcc lattice 12 first neighbors are equidistant from any lattice site, the 12 lead atoms surrounding a given cadmium atom can be put on the surface of a sphere whose radius equals the minimum distance between neighboring atoms. This representation is given in Fig. 3(a). From the radius of this sphere, the lattice parameter of the Pb(Cd) crystal was derived. The value of 4.93 Å obtained from the holographic data is in very good agreement with the values determined in the usual way by x-ray and neutron diffraction measurements. In the course of mounting the sample its orientation, as previously determined during the check at Saclay, was lost. However, this orientation could later be reconstructed from the hologram using the following procedure. First, using a model calculation, the positions of the expected high intensity spots were obtained for an arbitrary orientation. Subsequently, coincidence of the measured and calculated spots was achieved by suitably rotating the z and y axes. Comparison with the model calculation showed the [001] direction of the lead crystal to have a declination angle from the z axis of the diffractometer of $\Theta = 59 \pm 3°$ and the initial value of the rotation about the φ_0 axis to be $\varphi_0 = 21 \pm 3°$. After completing the holography experiment, the gamma detectors were removed and the diffractometer was used

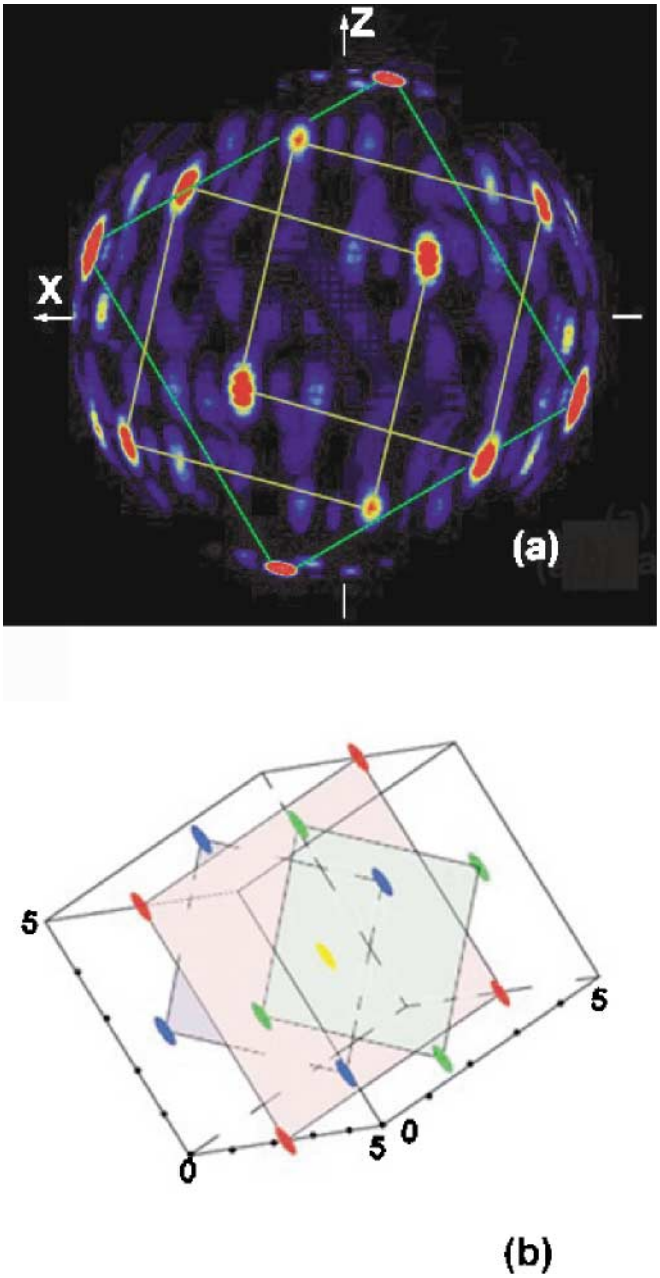

FIG. 3 (color). (a) The spots representing the positions of the twelve Pb atoms forming the first neighbors of the Cd nucleus are displayed on the surface of a sphere of radius 3.49 Å = $a/\sqrt{2}$, a being the lattice parameter. The x axis is the incident beam direction; the z axis is the z direction in the system of coordinates of the D9 diffractometer. (b) Schematic illustration of the arrangement of the lead atoms surrounding a Cd atom (yellow spot) as first neighbors in the fcc structure. The orientation and positions of the spots are equivalent to those in (a). The fcc cubic lattice, however, is tilted with respect to the z axis of the diffractometer according to the angles given in the text. The grid marks are given in angstroms.

in the usual way to measure several Bragg reflections of our sample. From these Bragg positions, the orientation matrix of the sample can be derived [7] finally yielding

both the angle between the z axes of the sample crystal and the diffractometer and the azimuthal rotation. This calculation gives the values $\Theta = -60.3°$ and $\varphi_0 = 20.3°$, in good agreement with the holographic data thereby demonstrating the power of the technique. To give a clearer view of the atomic arrangement, the image of the crystal in Fig. 3(a) has been rotated in such a way that the [001] direction becomes aligned with the z axis of the diffractometer, thus making both the interplanar and interatomic distances visible. Figure 3(b) shows the schematic view of the nuclei arranged in the fcc lattice. We emphasize that due to the nuclear interaction of neutrons these distances reflect the positions of neighboring nuclei in contrast to the case of x-rays where interatomic distances are defined by the interaction with the electronic shell.

To our knowledge, this work is the first in which the internal-detector concept was successfully realized for neutron holography, and the object was restored without making use of any *a priori* knowledge about the orientation of the sample. These results have demonstrated the feasibility of atomic resolution neutron holography as proposed in Ref. [4] is now proven and, on the basis of these results, practical applications appear highly promising. It would also be seen that the special properties of the nuclear scattering process of neutrons, including its isotopic sensitivity and its dependence on the magnetic moment, will substantially enlarge the field of investigation opened up by this novel technique of which we briefly mention just two examples: First, as already discussed in more detail [8], the internal-source concept is applicable to the investigation of a wide variety of hydrogen-containing compounds, both inorganic and organic. Second, by using polarized neutron beams, both the internal-source and the internal-detector concepts may be extremely useful and flexible tools for studying the local magnetic structure of magnetic materials.

The authors acknowledge the intellectual contribution and technical assistance of J. Allibon, J. Archer, M. Kocsis, J. Laugier, Ch. Ling, A. Pastor, M. Prem, Yu. Tolmachev, and G. Vaspál.

[1] D. Gabor, Nature (London) **161**, 777 (1948).
[2] A. Szöke, in *Short Wavelength Coherent Radiation: Generation and Applications*, edited by D.T. Attwood and J. Baker, AIP Conf. Proc. No. 147 (AIP, New York, 1986).
[3] M. Tegze and Gy. Faigel, Nature (London) **380**, 49 (1996).
[4] L. Cser, G. Krexner, and Gy. Török, Europhys. Lett. **54**, 747 (2001).
[5] B. Sur, R. B. Rogge, R. P. Hammond, V. N. P. Anghel, and J. Katsaras, Nature (London) **414**, 525 (2001).
[6] J. Dutkiewicz, Z. Moser, and W. Zakulsky, Bull. Alloy Phase Diagrams **9**, 694 (1988).
[7] W. R. Busing and H. A. Levy, Acta Crystallogr. **22**, 457 (1967).
[8] L. Cser, G. Krexner, and Gy. Török, Appl. Phys. A (to be published).